

OPEN

Generation of the *Fip111–Pdgfra* fusion gene using CRISPR/Cas genome editing

Leukemia (2016) **30**, 1913–1916; doi:10.1038/leu.2016.62

The *FIP1L1–PDGFRA* fusion gene is an important oncogenic driver of chronic eosinophilic leukemia, now referred to as the WHO subcategory 'myeloid and lymphoid neoplasms with eosinophilia and abnormalities of *PDGFRA*, *PDGFRB* or *FGFR1*'.^{1,2} The *FIP1L1–PDGFRA* fusion is generated by a 800-kb chromosomal deletion, unlike the majority of other fusion genes that are generated by chromosomal translocations. The resulting FIP1L1–PDGFRa protein (Figure 1a) is a constitutive active tyrosine kinase that is highly sensitive to the kinase inhibitor imatinib, and treatment with this drug results in rapid complete remission for *FIP1L1–PDGFRA* positive patients.³ Although the response to imatinib is excellent, most patients require life-long treatment and the development of resistance has been described in some cases.^{1,4,5}

Most of our insight into the mechanism of activation of the FIP1L1–PDGFRa kinase, its downstream signaling and its sensitivity to kinase inhibitors has been obtained from studies using ectopic overexpression of the recombinant fusion protein in Ba/F3 cells or other cell lines such as HEK293T. The interleukin-3 (IL-3)-dependent Ba/F3 cell line has been widely used to study oncogenic tyrosine kinases, since many constitutively activated tyrosine kinases can transform the Ba/F3 cells to IL-3-independent growth.^{1,6,7} It is at present unknown if the data obtained from such overexpression experiments is completely valid and if it accurately resembles the actual situation in the leukemia cells in which there is only one copy of the *FIP1L1–PDGFRA* gene driven by the *FIP1L1* promoter.

To address this question, we used CRISPR/Cas genome editing to generate the *Fip111–Pdgfra* fusion gene by inducing a 600-kb interstitial chromosomal deletion in the Ba/F3 cell line.⁸ We designed six different guide RNAs (gRNAs) targeting exons 9, 10, 11 or 12 of *Fip111* and three different gRNAs targeting exon 12 of *Pdgfra*, reflecting similar breakpoints found in *FIP1L1–PDGFRA* positive patients¹ (Figure 1b). The design tool developed by the Zhang lab (crispr.mit.edu) was used to find gRNAs with minimal off-target effects.⁹ gRNA sequences were cloned into a plasmid (pX330) carrying a Cas9 expression cassette, and this plasmid was delivered into Ba/F3 cells by electroporation. The targeting efficiency of the individual gRNAs in Ba/F3 cells was determined using next-generation sequencing. Using the same strategy, the frequency of insertions/deletions was determined for the top-4 genomic off-target locations as predicted by the design tool. Typically, we observed an on-target targeting efficiency between 8 and 55%, while for off-target locations the observed indel frequency was below 0.005% (Figure 1c).

To generate various *Fip111–Pdgfra* fusion genes (designated FP1 to FP6), we combined a gRNA targeting an exon of *Fip111* with a gRNA targeting exon 12 of *Pdgfra*. Upon IL-3 removal, only Ba/F3 cells that had generated an oncogenic Fip111–Pdgfra fusion protein were able to survive and proliferate in the absence of IL-3 (Figure 1d). The presence of the fusion gene and protein was confirmed by PCR and western blotting, respectively (Figures 1e and f).

Single cell clones were generated from the Ba/F3 cells harboring the six different *Fip111–Pdgfra* fusions using semi-solid growth medium (Clonacell, Stem Cell Technologies, Vancouver, BC, Canada). The region spanning the fusion between *Fip111* and *Pdgfra* was amplified by PCR and sequenced using Sanger sequencing (Figure 1g). Fluorescence *in situ* hybridization (FISH) confirmed the presence of the deletion between *Fip111* and *Pdgfra* on one copy of mouse chromosome 5 and we consistently only observed heterozygous deletions (Figure 1h). These data confirm that the *Fip111–Pdgfra* fusion gene can be generated by CRISPR/Cas genome editing and that expression of the fusion gene is sufficient to transform Ba/F3 cells in a similar manner to ectopic overexpression of the recombinant *FIP1L1–PDGFRA* fusion.

We showed previously that the Fip111 portion of the Fip111–Pdgfra fusion protein is dispensable for its transforming capacities.¹⁰ We have to note, however, that this was only studied under overexpression conditions.¹⁰ Using the genome editing strategy, we now generated a fusion between *Fip111* exon 1 and *Pdgfra* exon 12 (designated FP7), using gRNAs F7+P3 (Figure 1b). This strategy generated a fusion protein, as shown in Figure 2a, which was able to transform the cells, confirming that also with normal expression levels, the Fip111 part is dispensable for constitutive kinase activation (Figures 2b–d).

We also showed previously that disruption of the juxtamembrane domain of *Pdgfra* (exon 12), removing one of the conserved tryptophan residues responsible for autoinhibition of the JM domain, is absolutely required for the transforming capacities of the fusion protein.¹⁰ To confirm these earlier findings with more normal expression levels, we used the same genome editing strategy to generate a Fip111–Pdgfra fusion protein with an intact juxtamembrane domain (Figure 2e). We designed four different gRNAs targeting intron 10 of *Pdgfra* (designated P4a–d, Figure 1b), from which three gRNAs were able to generate a fusion gene in combination with a gRNA targeting *Fip111* (Figure 2f, the four different fusions are designated FP9-1 to FP9-4). However, these fusion proteins were not able to transform Ba/F3 cells (Figure 2g). These data show that Fip111 is dispensable for the transformation capacities of the Fip111–Pdgfra fusion protein, and that interruption of the juxtamembrane domain is critical for the activation of the Fip111–Pdgfra protein. Taken together, these results show that previously obtained data with overexpression models are valid.

Next, we compared the expression and phosphorylation levels of Fip111–Pdgfra between the CRISPR/Cas-generated Ba/F3 cells harboring the endogenous *Fip111–Pdgfra* fusion gene and retrovirally transduced cells overexpressing *FIP1L1–PDGFRA*. Retrovirally transduced cells showed more than 10-fold higher protein expression and phosphorylation levels of FIP1L1–PDGFRa, as calculated by ImageJ software. We observed similar expression and phosphorylation of Stat5, which is a downstream effector of Fip111–Pdgfra (Figure 2h). When the cells were treated with 100 nM imatinib, the autophosphorylation of Fip111–Pdgfra was completely inhibited (Figure 2h). Remarkably, the EC50 values (measured after 24 h exposure to Imatinib) were not significantly different between the CRISPR/Cas-generated Ba/F3 cells and retrovirally transduced cells (95% confidence intervals for the EC50 values shown in Figure 2i). These results show that, despite

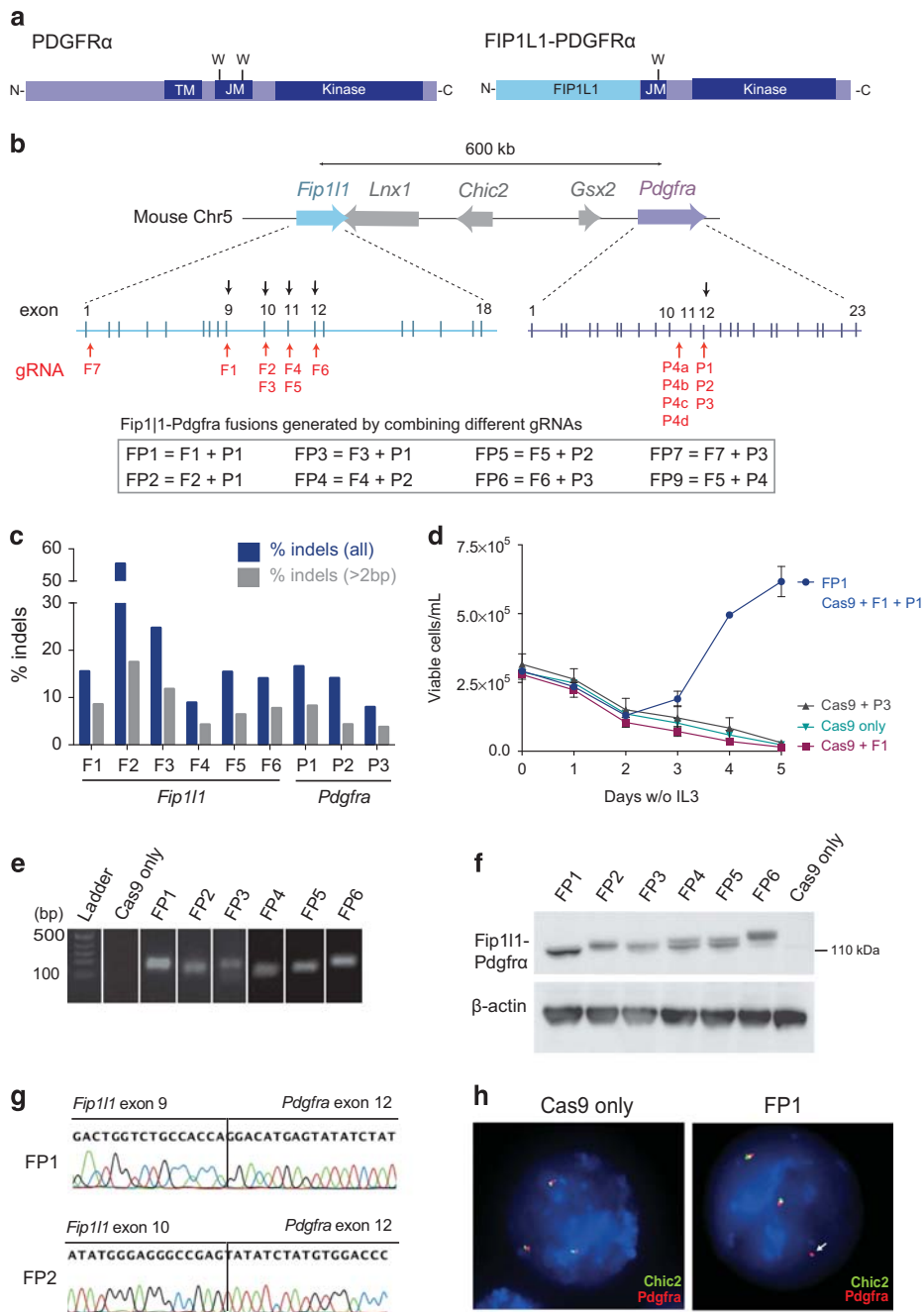


Figure 1. Use of CRISPR/Cas genome editing to generate Fip111-Pdgfra fusions. **(a)** Structure of PDGFR α and the FIP1L1-PDGFR α fusion protein. Formation of the fusion leads to disruption of the JM domain between two tryptophan (W) residues in PDGFR α (TM = transmembrane domain, JM = juxtamembrane domain). **(b)** Representation of the *Fip111* and *Pdgfra* mouse genes. Exons are indicated by vertical bars. Red arrows indicate the location of the gRNA target sites in mouse *Fip111* and *Pdgfra*. Black arrows indicate homologous sequences of breakpoints found in patients. **(c)** Efficiency of the individual gRNAs targeting *Fip111* and *Pdgfra* in Ba/F3 cells as determined by Illumina next-generation sequencing. **(d)** Growth curve showing the transforming capacities of Ba/F3 cells harboring an endogenous FP1 fusion. Ba/F3 cells harboring a FP2–FP6 fusion had similar transformation rates (data not shown). Electroporation of only 1 gRNA targeting *Fip111* or *Pdgfra* could not transform the Ba/F3 cells. Cas9 only refers to a vector containing Cas9 without a gRNA sequence. **(e)** PCR to detect six different gene fusions in Ba/F3 cells electroporated with a vector containing Cas9 and gRNA sequences targeting *Fip111* and *Pdgfra*. Cas9 only refers to a vector containing Cas9 without a gRNA sequence. **(f)** Western blot showing six different Fip111-Pdgfra fusion proteins expressed in Ba/F3 cells. Different breakpoints in *Fip111* lead to different molecular weights. **(g)** Sequencing trace showing a fusion between *Fip111* and *Pdgfra* in Ba/F3 single cell clones of two different fusion genes (FP1 and FP2). **(h)** FISH on Ba/F3 cells electroporated with empty vector or with vectors containing *Fip111*-*Pdgfra* gRNAs. The white arrow indicates loss of one copy of *Chic2*, a gene in the deleted region between *Fip111* and *Pdgfra*.

the more than 10-fold difference in protein expression levels, the sensitivity of the cells to imatinib was not significantly altered.

Overall, these data show that it is feasible to generate fusion genes in the IL3-dependent Ba/F3 cell line using CRISPR/Cas

genome editing, and that these fusion genes can transform the cells to IL3-independent growth. We also conclude that no major differences were observed between Ba/F3 cells overexpressing FIP1L1-PDGFR α from a retroviral construct and CRISPR/Cas

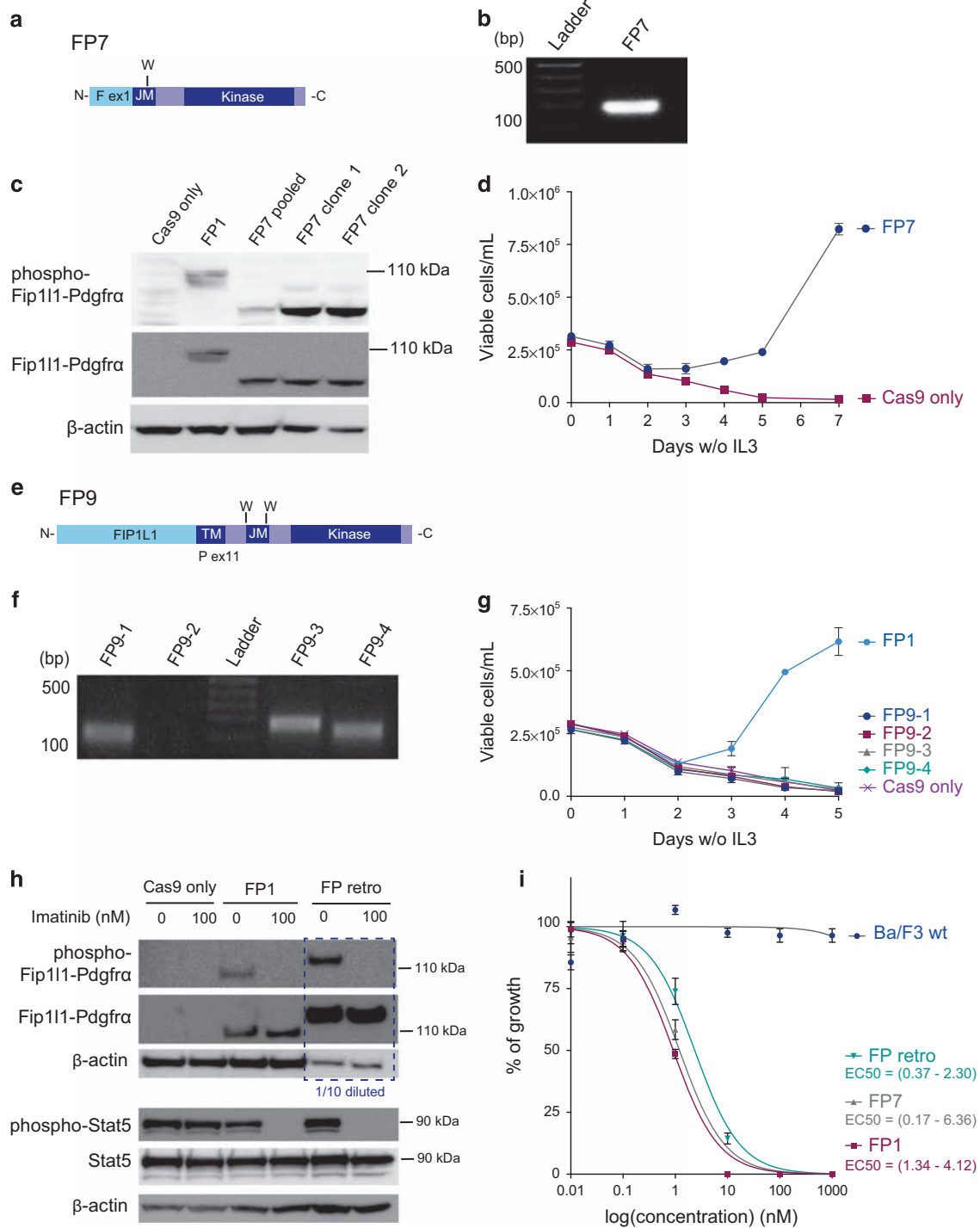


Figure 2. Study of the properties of the Fip111-Pdgfra fusion protein. **(a)** Structure of the FP7 fusion. Break points are located in *Fip111* exon 1 and *Pdgfra* exon 12 (W = tryptophan residue, TM = transmembrane domain, JM = juxtamembrane domain). **(b)** PCR to detect the FP7 fusion in Ba/F3 cells. **(c)** Western blot showing expression of the FP7 fusion protein in Ba/F3 cells after electroporation of gRNAs targeting *Fip111* exon 1 and *Pdgfra* exon 12. **(d)** Growth curve showing the transforming capacities of Ba/F3 cells harboring an endogenous FP7 fusion. **(e)** Structure of the FP9 fusion. Break points are located in *Fip111* exon 9 and *Pdgfra* exon 11 (W = tryptophan residue, TM = transmembrane domain, JM = juxtamembrane domain). **(f)** PCR to detect four different FP9 fusions with four different gRNAs targeting the upstream region of *Pdgfra* exon 11. **(g)** Growth curve of Ba/F3 cells harboring an endogenous FP1 or FP9 fusion. **(h)** Western blot showing the effects of Imatinib on the Fip111-Pdgfra fusion protein. Ba/F3 cells harboring an endogenous FP1 fusion (FP1) and Ba/F3 cells expressing a human FIP1L1-PDGFR α cDNA (FP retro) were treated for 90 min with 0 or 100 nM Imatinib. On the blots showing expression of (p)-Fip111-Pdgfra, a 1/10 dilution of FP retro is shown. Difference in molecular weight of Fip111-Pdgfra is due to differences in molecular weight between the mouse and human fusion proteins. **(i)** Dose response curve for Imatinib. EC50 values are represented by 95% confidence intervals.

engineered cells. The cells equally activated the downstream effector Stat5, and were equally sensitive to imatinib, despite the huge differences in protein expression levels. Moreover, previous data on the mechanism of activation were confirmed in the CRISPR/Cas engineered cells. Our data demonstrate an important application of the CRISPR/Cas genome editing tool, which makes it possible to study the oncogenic properties of activated tyrosine kinases without the need for ectopic overexpression.

CONFLICT OF INTEREST

The authors declare no conflict of interest.

ACKNOWLEDGEMENTS

This work was supported by the Stichting Tegen Kanker (JC), KU Leuven (JC, IW), and the Agency for Innovation by Science and Technology in Flanders – IWT (MVB).

M Vanden Bempt^{1,2}, S Demeyer^{1,2}, N Mentens^{1,2}, E Geerdens^{1,2},
CE De Bock^{1,2}, I Wlodarska¹ and J Cools^{1,2}

¹KU Leuven Center for Human Genetics, Leuven, Belgium and
²VIB Center for the Biology of Disease, Leuven, Belgium
E-mail: jan.cools@med.kuleuven.be

REFERENCES

- Cools J, DeAngelo DJ, Gotlib J, Stover EH, Legare RD, Cortes J *et al.* A tyrosine kinase created by fusion of the PDGFRA and FIP1L1 genes as a therapeutic target of imatinib in idiopathic hypereosinophilic syndrome. *N Engl J Med* 2003; **348**: 1201–1214.
- Tefferi A, Vardiman JW. Classification and diagnosis of myeloproliferative neoplasms: the 2008 World Health Organization criteria and point-of-care diagnostic algorithms. *Leukemia* 2008; **22**: 14–22.
- Jovanovic JV, Score J, Waghorn K, Cilloni D, Gottardi E, Metzgeroth G *et al.* Low-dose imatinib mesylate leads to rapid induction of major molecular responses and achievement of complete molecular remission in FIP1L1-PDGFRα-positive chronic eosinophilic leukemia. *Blood* 2007; **109**: 4635–4640.
- Lierman E, Michaux L, Beullens E, Pierre P, Marynen P, Cools J *et al.* FIP1L1-PDGFRα D842V, a novel panresistant mutant, emerging after treatment of FIP1L1-PDGFRα T674I eosinophilic leukemia with single agent sorafenib. *Leukemia* 2009; **23**: 845–851.
- von Bubnoff N, Sandherr M, Schlimok G, Andreesen R, Peschel C, Duyster J. Myeloid blast crisis evolving during imatinib treatment of an FIP1L1-PDGFRα-positive chronic myeloproliferative disease with prominent eosinophilia. *Leukemia* 2005; **19**: 286–287.
- Gorantla SP, Zirikli K, Reiter A, Yu C, Illert AL, Von Bubnoff N *et al.* F604S exchange in FIP1L1-PDGFRα enhances FIP1L1-PDGFRα protein stability via SHP-2 and SRC: a novel mode of kinase inhibitor resistance. *Leukemia* 2015; **29**: 1763–1770.
- von Bubnoff N, Gorantla SP, Engh RA, Oliveira TM, Thöne S, Aberg E *et al.* The low frequency of clinical resistance to PDGFR inhibitors in myeloid neoplasms with abnormalities of PDGFRα might be related to the limited repertoire of possible PDGFRα kinase domain mutations in vitro. *Oncogene* 2011; **30**: 933–943.
- Doudna JA, Charpentier E. The new frontier of genome engineering with CRISPR-Cas9. *Science* 2014; **346**: 1258096–1258096.
- Ran FA, Hsu PD, Wright J, Agarwala V, Scott DA, Zhang F. Genome engineering using the CRISPR-Cas9 system. *Nat Protoc* 2013; **8**: 2281–2308.
- Stover EH, Chen J, Folens C, Lee BH, Mentens N, Marynen P *et al.* Activation of FIP1L1-PDGFRα requires disruption of the juxtamembrane domain of PDGFRα and is FIP1L1-independent. *Proc Natl Acad Sci USA* 2006; **103**: 8078–8083.



This work is licensed under a Creative Commons Attribution-NonCommercial-ShareAlike 4.0 International License. The images or other third party material in this article are included in the article's Creative Commons license, unless indicated otherwise in the credit line; if the material is not included under the Creative Commons license, users will need to obtain permission from the license holder to reproduce the material. To view a copy of this license, visit <http://creativecommons.org/licenses/by-nc-sa/4.0/>

Donor cell leukemia arising from clonal hematopoiesis after bone marrow transplantation

Leukemia (2016) **30**, 1916–1920; doi:10.1038/leu.2016.63

Alterations in genes encoding epigenetic regulators are common in myeloid malignancies, and several recent studies have demonstrated that these mutations are present at high frequencies within peripheral blood cells in ~10% of individuals over 60 years of age. Although the presence of these mutations carries an increased risk of subsequent hematologic malignancies, the vast majority of individuals do not progress clinically and the natural history of clonal hematopoiesis is unclear.^{1–3} Thus, the term Clonal Hematopoiesis of Indeterminate Potential (CHIP) was proposed.⁴

Allogeneic bone marrow transplantation (alloBMT) remains the only curative therapy for many patients with hematologic malignancies. Over the past decade, advances in alloBMT have permitted older patients to successfully undergo the procedure. Accordingly, older matched sibling donors are being utilized. Moreover, the development of safe and effective haploidentical BMT allows parents to serve as related donors for their children.⁵ We hypothesized that clinically silent ‘pre-malignant’ clones (which do not result in overt malignancy under homeostatic conditions

within the donor) may be subjected to substantial proliferative and self-renewal stress during the engraftment process and could undergo transformation. We report two cases of donor cell leukemia (DCL) arising from CHIP marked by somatic mutations in leukemia-related genes in donors over age 60 years.

The study was approved by the Institutional Review Board at the Johns Hopkins University. Clonality was detected by a custom leukemia DNA sequencing panel covering 637 genes important in oncogenesis (Supplementary Methods).

From 2011 to 2014, we used 61 bone marrow donors >60 years-of-age at our institution (Supplementary Table 1). Median and maximum follow-up were 389 and 1481 days, respectively. Two recipients developed DCL for a cumulative incidence of 6.3% (95% confidence intervals: 0.94%, 19.6%). Donors and recipients characteristics are given in Supplementary Tables 1 and 2. Patient 1 was diagnosed with therapy-related AML and received two rounds of induction chemotherapy followed by myeloablative, haploidentical allo-BMT from his 68-year-old mother. The patient's course was complicated by primary graft failure and he subsequently underwent salvage nonmyeloablative haploidentical peripheral blood stem cell transplantation from the same donor. The bone marrow biopsy at 2.5 years showed focal erythroid dysplasia and no increased blasts (Supplementary Figure 1a). His